Multilinear Regression Equations for Predicting Lateral Spread Displacement from Soil Type and CPT Data

Citation	Gillins, D. T., & Bartlett, S. F. (2014). Multilinear Regression Equations for Predicting Lateral Spread Displacement from Soil Type and Cone Penetration Test Data. Journal of Geotechnical and Geoenvironmental Engineering, 140(4). doi:10.1061/(ASCE)GT.1943-5606.0001051
DOI	10.1061/(ASCE)GT.1943-5606.0001051
Publisher	ASCE - American Society of Civil Engineers
Version	Accepted Manuscript
Terms of Use	http://cdss.library.oregonstate.edu/sa-termsofuse

Multilinear Regression Equations for Predicting Lateral Spread Displacement from Soil Type and CPT Data

Daniel T. Gillins, Ph.D., M.ASCE[1]; and Steven F. Bartlett, Ph.D., M.ASCE[2]

Abstract: In the 1990s, Bartlett and Youd introduced empirical equations for predicting horizontal displacement from liquefaction-induced lateral spreading; these equations have become popular in engineering practice. The equations were developed by multilinear regression (MLR) of lateral spreading case history data compiled by these researchers. In 2002, these equations were revised and updated to include additional case history data. The regressions indicated that the amount of horizontal displacement is statistically related to the topography, earthquake magnitude, and distance from the seismic energy source; and, the thickness, fines content, and mean grain size of the saturated, granular sediments with corrected Standard Penetration Test blow count values less than 15. This paper proposes to modify the MLR empirical equations by replacing the fines content and mean grain size factors with soil description factors. Such modification allows investigators performing preliminary evaluations to make lateral spread displacement estimates using existing geotechnical data with sparse laboratory measurements. The paper also proposes a methodology to estimate the required geotechnical inputs in the proposed modified MLR equations using cone penetration test data.

CE Database subject headings: Soil liquefaction; Lateral displacement; Earthquakes; Empirical equations; Penetration tests; Cone penetration tests

[1] Assistant Professor, School of Civil & Construction Engr., Oregon State Univ., 220 Owen Hall, Corvallis, OR 97331; e-mail: dan.gillins@oregonstate.edu
[2] Associate Professor, Dept. of Civil & Environ. Engr., Univ. of Utah, 110 Central Campus Dr., Salt Lake City, UT 84112; e-mail: bartlett@civil.utah.edu

Introduction

Lateral spread is a pervasive type of liquefaction-induced ground failure generated by moderate to large-sized earthquakes (NRC 1985). During lateral spread, blocks of mostly intact, surficial soil atop a liquefied layer displace down slope on topography as gentle as 0.5% slope, or towards a free-face, such as a river channel or bluff. This type of ground failure can involve large areas and produce horizontal displacements up to several meters, resulting in considerable damage to bridges, buildings, pipelines, roadways, and other constructed works. During some earthquakes, such as the 1964 Alaska earthquake, ground failures from lateral spreading accounted for the majority of the earthquake damage (Bartlett and Youd 1992). When studying areas prone to liquefaction, it is important to evaluate the lateral spread hazard.

Lateral spread is a complex, dynamic, natural phenomenon, requiring investigators to: (1) assess topographic conditions, (2) account for variations in the underlying soil profile and its properties, (3) evaluate liquefaction susceptibility, and (4) estimate the potential ground displacement for a highly nonlinear, dynamic process. Due to these and other complexities, many researchers have developed empirical or semiempirical equations to estimate horizontal displacements from lateral spreads (e.g., Hamada et al. 1986, Youd and Perkins 1987, Rauch and Martin 2000, Bardet et al. 2002, Baska 2002, Youd et al. 2002, Zhang et al. 2004, Faris et al. 2006, Olson and Johnson 2008). For the most part, these researchers derived their equations from statistical regression techniques of compiled case histories of liquefaction-induced lateral spread.

Bartlett and Youd (1992; 1995) introduced such empirical equations for predicting the amount of horizontal displacement from liquefaction-induced lateral spreading; these equations have become popular in engineering practice. The equations were developed by multilinear

regression (MLR) of a large lateral spread case history database compiled by these researchers. Later, Youd et al. (2002) corrected some errors in the MLR case history database, added case history data from three additional earthquakes, and presented revised MLR equations. The regressions indicated that the amount of horizontal displacement from lateral spreading is statistically correlated with the ground slope or proximity to and depth of a nearby free-face, moment magnitude of the earthquake, and distance from the seismic energy source; and, the thickness, fines content, and mean grain size of the saturated, granular sediments with Standard Penetration Test (SPT) $N_{1,60}$ values less than 15 (Bartlett and Youd, 1992).

In general, investigators of a site will determine the geotechnical factors for the Youd et al. (2002) MLR empirical equations by performing SPT(s) and soil gradation tests in the laboratory. However, some investigators engaged in performing large-scale (e.g., regional hazard mapping) or preliminary studies may wish to use existing geotechnical borehole data to estimate lateral spread displacements. This situation is addressed by this paper and the MLR models proposed herein.

Often during routine drilling and sampling investigations not directed specifically at liquefaction assessment, practitioners will commonly report the soil description, layer thickness and corresponding SPT blow count (N) values. However, laboratory-determined mean grain size and fines content data are rarely measured or reported. For example, while assessing the lateral spread hazard for a large study area in Weber County, Utah, we gathered 251 soil/SPT borehole logs from local municipalities, county offices, private engineering firms, and state governments (Bartlett and Gillins, 2013). Unfortunately, none of these borehole logs and their associated geotechnical reports listed values of mean grain size; and, few of these logs listed fines content information for the potentially liquefiable layer(s).

To address this issue regarding lack of data in the existing borehole logs, Bardet et al. (2002) suggested removing the fines content and mean grain size variables from the MLR equations. Although removal of these variables simplifies the data requirements in the MLR equations, such removal introduces more uncertainty in the lateral spread displacement estimates. Olsen et al. (2007) suggested estimating missing measurements of mean grain size and fines content by using average values from other borehole studies with similar soil type and geology. However, such averaging removes variability and adds uncertainty that is difficult to quantify to the displacement estimates.

To resolve this missing data issue, this paper proposes to modify the Youd et al. (2002) MLR equations by replacing the fines content and mean grain size factors with soil description factors. The proposed modification is not meant to replace or improve upon the Youd et al. (2002) MLR equations. Rather, this modification is intended to provide a method for estimating lateral spread displacement from existing borehole data that lack or have sparse laboratory measurements. Displacement estimates from the proposed MLR equations will aid investigators in deciding if new drilling and sampling is warranted in order to further reduce the uncertainties in the subsurface, and improve the precision of the lateral spread displacement estimates. This paper will show that the modified MLR empirical equations: (1) are reasonably reliable, as judged by a comparison of the statistical performance of the proposed model with the MLR model of Youd et al. (2002), (2) have better statistical performance than MLR equations that simply remove the fines content and mean grain size variables from the MLR model; and (3) have geotechnical inputs that may be reasonably estimated from Cone Penetration Test (CPT) results.

The Youd et al. (2002) MLR Model

Eqn. (1) lists the general form of the Youd et al. (2002) MLR model.

$$LogD_H = \begin{matrix} b_o + b_{off}\alpha + b_1 M + b_2 LogR^* + b_3 R + b_4 LogW + b_5 LogS + b_6 LogT_{15} + \\ + b_7 Log(100 - F_{15}) + b_8 Log(D50_{15} + 0.1\ \text{mm}) \end{matrix} \quad (1)$$

where D_H is the estimated horizontal displacement (m) from lateral spreading; M is the moment magnitude of the earthquake (M_w); R is the nearest horizontal or mapped distance from the site to the seismic energy source (km); and, R^* is a nonlinear magnitude-distance function calculated by eqn. (2).

$$R^* = R + 10^{0.89 \cdot M - 5.64} \quad (2)$$

W is the ratio of the height of the free face to the horizontal distance between the base of the free face and the point of interest (%); S is the ground slope (%); T_{15} is the cumulative thickness (m) of saturated, cohesionless deposits in the soil profile with corrected Standard Penetration Test (SPT) blows counts, $N_{1,60} \leq 15$; F_{15} is the average fines content (percentage of sediment passing a No. 200 sieve) of the materials comprising T_{15} (%); $D50_{15}$ is the average mean grain size of the materials comprising T_{15} (mm); and, α is a dummy variable defining the controlling topographic conditions at the point of interest. For sloping-ground conditions, α is set to zero, W is set to 1, and site-specific estimates of *S (%)* are entered. For free-face conditions, α and S are set to 1, and site-specific values of *W (%)* are entered. Youd et al. (2002) computed the following partial regression coefficients for eqn. (1): b_o = -16.213, b_{off} = -0.500, b_1 = 1.532, b_2 = -1.406, b_3 = -0.012, b_4 = 0.592, b_5 = 0.338, b_6 = 0.540, b_7 = 3.413, and b_8 = -0.795.

The linear relationship between the dependent variable and independent variables in eqn. (1) can be evaluated by a statistical hypothesis test named Analysis of Variance (ANOVA). Statistical hypothesis testing involves assuming a null hypothesis, and testing it for statistical significance. Statisticians decide to reject the null hypothesis when the probability (i.e., *P*-value) of exceeding the result of the hypothesis test is less than a predetermined threshold or significance level. Commonly, statisticians set 5% as a level of significance for deciding if the null hypothesis should be rejected. ANOVA for linear regression tests the null hypothesis that the variance of the data explained by the model is equal to the variance of the data not explained by the model. The ratio of these respective variances, or *F*-statistic, follows a Fisher distribution. Table 1 summarizes the ANOVA results for the Youd et al. (2002) MLR model. As can be seen, the *F*-statistic is equal to 267.9, indicating that the variance of the data explained by the model is much greater than the variance of the data not explained by the model; and, the probability of exceeding this *F*-statistic is essentially zero (i.e., *P*-value $\approx$ 0). Since the *P*-value is less than 0.05, we reject the null hypothesis at the 5% significance level, and conclude that a linear relationship exists between the dependent variable and the independent variables in the Youd et al. (2002) MLR model. The coefficient of determination for this model, R^2, is 83.6%; the adjusted R^2 is 83.3%; and, the standard deviation of the predicted variable, σ_{logDH}, is 0.1970.

Modifications to the Youd et al. (2002) Model

As discussed in the introduction of this paper, to address the common issue of lack of available F_{15} and $D50_{15}$ data from record SPT boreholes, Bardet et al. (2002) have suggested MLR empirical models that do not include these variables. After removal of the F_{15} and $D50_{15}$ variables from eqn. (1), the reduced empirical model has the general form shown in eqn. (3).

$$LogD_H = b_o + b_{off}\alpha + b_1 M + b_2 LogR^* + b_3 R + b_4 LogW + b_5 LogS + b_6 LogT_{15} \quad (3)$$

Upon regression of the case history database compiled by Youd et al. (2002), eqn. (3) has the following partial regression coefficients: b_o = -9.087, b_{off} = -0.353, b_1 = 1.428, b_2 = -0.902, b_3 = -0.020, b_4 = 0.401, b_5 = 0.293, and b_6 = 0.560. Table 2 summarizes the ANOVA results for eqn. (3). Although the *P*-value for this statistical hypothesis test remains much less than the 5% significance level, R^2 for the reduced model has decreased to 66.6%; indicating only 66.6% of the variability in the dependent variable, *Log* D_H, is explained by the independent variables. Also, the *F*-statistic decreased to 135.7, adjusted R^2 decreased to 66.1%, the variance of the regression equation as indicated by the mean squared error (i.e., *MSE*) has more than doubled that of the Youd et al. (2002) MLR model, and the standard deviation of the predicted variable, σ_{logDH}, has increased to 0.2802.

Figure 1a depicts predicted values of D_H from eqn. (3) versus measured values of D_H from the case history database of Youd et al. (2002). The solid line on the plot (that is at 45 degrees from the origin) represents a perfect prediction line or a mean-estimate line. Points plotting near this line represent displacements that are closely predicted by the model. The dashed lines, plotted at 2:1 and 1:2 slopes, represent a 100% over-prediction boundary and a 50% under-prediction boundary, respectively. Points plotting above or below these bounds represent displacements that are being either over or under-predicted by a factor of 2 or greater. Figure 1a shows that 18.6% (90 out of 484) of the displacements predicted by eqn. (3) fall outside these bounds—of which many fall well outside the bounds. Other points in Figure 1a, as grouped and symbolized by earthquake, also trend in one direction, either consistently above or

below the 1:1 line. For instance, eqn. (3) heavily over-predicts all of the displacements recorded for the 1964 Alaska earthquake. Instead of following the 1:1 line, these points plot along a line approximately 80 degrees left of the horizontal axis.

Because of the overall lack of fit of eqn. (3), it is desirable to seek other variables to replace F_{15} and $D50_{15}$ in the empirical model. We found that recorded SPT borehole logs often include a description of the soil along with the corresponding SPT N values. Such soil descriptions are also found in the borehole logs in the MLR case history database, and we wanted to test if these descriptions might be used to improve the performance of eqn. (3). For an example of how we started our analysis, Figure 2 shows a plot of borehole data at a site in Alaska from the MLR case history database compiled by Bartlett and Youd (1992). This figure shows SPT $N_{1,60}$ values and corresponding soil descriptions at a site with groundwater located near the surface. The five shaded layers indicate zones that are cohesionless, saturated, and have values of $N_{1,60} \leq 15$. The sum of the thickness of these 5 layers, T_{15}, is equal to 20.6 meters. T_{15} layers like those shown in Figure 2 can be found for every T_{15} value in the Youd et al. (2002) lateral spread database.

We assigned a soil index, *SI*, to each T_{15} layer according to the most general description of the soil from the boring log. Prior to doing so, we checked the MLR database for consistency between the soil description and the recorded values of fines content and mean grain size to ensure no significant errors in the description existed. Only 2.5% of all T_{15} layers in the MLR database were described incorrectly, according to corresponding measurements of mean grain size and fines content; we corrected the soil descriptions for these layers. Primarily, these few description errors were between silty sands (SM) and sandy silts (ML) where the amount of sand and silt were similar. Table 3 groups the soil descriptions by assigned values of *SI*, and lists for

each group the corresponding number (n) of SPT boreholes in the 2002 MLR case history database, the mean and standard deviation of the mean grain size ($\overline{D50}$ and $\sigma_{D50,}$ respectively), and the mean and standard deviation of the fines content ($\overline{FC}$ and $\sigma_{FC,}$ respectively). In order to complete the definition of SI for each soil type, we assigned nonliquefiable material (i.e., highly cohesive soils) a value of SI = 6. Table 4 summarizes the number of ground displacement vectors per earthquake in the 2002 MLR case history database, and lists the number of SPT boreholes that identified T_{15} layers with values of SI = 1, 2, 3, 4, or 5. Only 5 SPT boreholes (4 from case history studies of the 1983 Borah Peak, Idaho, earthquake; 1 from the 1995 Kobe, Japan, earthquake) identified T_{15} layers with a value of SI = 1 (silty gravel, fine gravel). However, numerous SPT boreholes from case history studies of at least a few earthquakes found T_{15} layers ranging from silts to very coarse sands with gravel. As shown in Table 4, at least 34 SPT boreholes from at least 4 different earthquakes in the western United States or Japan identified T_{15} layers with values of SI = 2, 3, 4, or 5.

By including soil description variables in the MLR empirical model in lieu of the F_{15} and $D50_{15}$ variables, the modified model has the general form shown in eqn. (4).

$$LogD_H = \begin{array}{c} b_o + b_{off}\alpha + b_1 M + b_2 LogR^* + b_3 R + b_4 LogW + b_5 LogS + \\ + b_6 LogT_{15} + a_1 x_1 + a_2 x_2 + a_3 x_3 + a_4 x_4 + a_5 x_5 \end{array} \quad (4)$$

where x_i is the thickness of the layers in the site profile that comprise T_{15} with $SI = i$ divided by the total cumulative thickness of T_{15}, represented as a decimal. For example, the borehole plotted in Figure 2 has x_1 = 1.96 / 20.6 = 0.10; x_2 = 6.02 / 20.6 = 0.29; x_3 = 0.25; x_4 = 0.33; and, x_5 = 0.03. Of course, the sum of all values of x in the borehole equals 1.

206 Following the same technique as Bartlett and Youd (1992), we used an inverse-weighted
207 averaging scheme to assign computed values of x to every displacement vector. This averaging
208 scheme assigns the largest weight to the borehole located closest to the displacement location,
209 and decreasingly smaller weights to boreholes located at greater distances.

210 It is important to note that during least squares regression, R^2 will generally increase as
211 the number of independent variables increases, even if an additional independent variable is
212 hardly correlated with the predicted variable. Due to potential inflation of R^2, when comparing
213 models with different amounts of independent variables, it is better to compare F-statistics or
214 adjusted R^2 values. To avoid adding extra or unnecessary variables to the empirical model, we
215 began with eqn. (3) and added each new soil description (i.e., x_i) variable from eqn. (4) one step
216 at a time, performed the regression, and computed adjusted R^2. We added each of the x_i
217 variables in varying combinations, and found after every regression step that adjusted R^2
218 increased and never decreased. Since adjusted R^2 never decreased, we conclude that each of the
219 x_i variables are correlated with the predicted variable, and none are extra or inflate R^2.

220 Eqn. (4) has the following partial regression coefficients based on regression of the case
221 history database of Youd et al. (2002): b_o = -8.208, b_{off} = -0.344, b_1 = 1.318, b_2 = -1.073,
222 b_3 = -0.016, b_4 = 0.445, b_5 = 0.337, b_6 = 0.592, a_1 = -0.683, a_2 = -0.200, a_3 = 0.252, a_4 = -0.040, and
223 a_5 = -0.535. Table 5 summarizes the ANOVA results for eqn. (4). As can be seen, the F-statistic
224 increased to 148.0, and the P-value for this statistical hypothesis test remains much less than the
225 5%. This indicates that eqn. (4) is statistically significant for predicting the dependent variable,
226 $Log\ D_{H.}$ Moreover, the R^2 for this model is 79.0%, adjusted R^2 is 78.5%, and the standard
227 deviation of the predicted variable, σ_{logDH}, is 0.2232. These values are similar to those found for
228 the Youd et al. (2002) MLR model (eqn. (1)). For comparison, R^2 is only 4.6% less, and σ_{logDH} is

only 0.0262 more than the value found for eqn. (1). In addition, Figure 1b shows predicted values of D_H from eqn. (4) versus measured values of D_H from the case history database. Comparing this plot with Figure 1a, more points fall between the bounds of the 1:2 and 2:1 sloped lines (88.4% of the points compared to 81.4% in Figure 1a). These comparisons demonstrate that replacing the F_{15} and $D50_{15}$ variables with soil description variables in the MLR empirical model is an improvement over simply removing the F_{15} and $D50_{15}$ variables from the MLR model.

The values of the partial regression coefficients for the soil description variables indicate their relative influence on displacement. For example, the maximum of these coefficients is a_3, indicating that fine to medium-grained sands with low fines content are associated with larger lateral spread displacement than other soil types. Coarse grained material, especially gravels with sufficient fines content to impede drainage, have smaller coefficient values. Very fine-grained, granular materials, such as sandy silts, have a negative partial regression coefficient, which means they produce smaller displacements on average when compared with the mean estimate from the regression model.

To further show how soil type and thickness affect the amount of lateral spread displacement, the variable T_{15} can be adjusted to an equivalent "clean sand" value, $T_{15,cs}$. We define $T_{15,cs}$ as a T_{15} value for fine to medium-grained clean sand only, which occurs when x_3 = 1 and all other x's = 0. This new variable is calculated by using the final 6 terms in eqn. (4), as listed in eqn. (5).

$$b_6 Log T_{15} + [\mathbf{a}][\mathbf{x}] = b_6 Log T_{15} + a_1 x_1 + a_2 x_2 + a_3 x_3 + a_4 x_4 + a_5 x_5 \quad (5)$$

where [**a**] is a vector for a_1 through a_5, and [**x**] is a vector for x_1 through x_5. Inserting T_{15} = $T_{15,cs}$, $x_1 = x_2 = x_4 = x_5 = 0$, and $x_3 = 1$, into the right-hand side of eqn. (5) results in eqn. (6).

$$b_6 LogT_{15} + [\mathbf{a}][\mathbf{x}] = b_6 LogT_{15,cs} + a_3 \quad (6)$$

We solve for $T_{15,cs}$, as shown in eqn. (7).

$$T_{15,cs} = T_{15} \cdot 10 \wedge \left(\frac{[\mathbf{a}][\mathbf{x}] - a_3}{b_6} \right) \quad (7)$$

Values of $T_{15,cs}$ for a given borehole provide a single geotechnical variable that can be substituted into eqn. (4) for T_{15} (with $x_3 = 1$ and all other x 's = 0). Most of the ax terms in eqn. (4) are thereby removed, because their values of $x = 0$. Using a single regression variable also shows how soil type and thickness jointly affect lateral spread displacement. For example, Figure 3 shows values of $T_{15,cs}$ plotted versus T_{15} for various soil types. Holding all other independent variables in eqn. (4) constant (i.e., *M*, *R*, *W*, *S*), Figure 3 demonstrates that 1 meter of saturated, clean, fine to medium-grained sand with $N_{1,60} \leq 15$ has the same displacement potential as over 15 meters of saturated soil that is either gravel or silt with $N_{1,60} \leq 15$.

Discussion of the Modified MLR Model

The modified MLR equation (eqn. (4)) provides a method to estimate D_H from liquefaction-induced lateral spread using existing borehole data that, as is often the case, lack laboratory-determined measurements of $D50_{15}$ and F_{15}. Predictions from eqn. (4) are more

reliable than predictions obtained from eqn. (3) that omits these soil factors. We believe that investigators performing preliminary lateral spread evaluations from existing geotechnical data may find the modified MLR model useful for estimating horizontal displacement. In addition, preliminary estimates from eqn. (4) may aid investigators in deciding if new drilling, sampling, and testing information is needed based on the level of the predicted displacement and the level of uncertainty in their evaluations. If additional investigations are planned, we recommend that investigators obtain the data required for use in more detailed models, such as that proposed by Youd et al. (2002).

Both the Youd et al. (2002) MLR equation (eqn. (1)) and eqn. (4) predict lateral spread displacement using M, R, S, W, and T_{15}. However, predictions from eqn. (4) may have somewhat more uncertainty than those from eqn. (1) because eqn. (4) uses soil description variables (i.e., $x_1 - x_5$) in lieu of laboratory-determined input factors (i.e., $D50_{15}$, F_{15}). Inherent in the use of eqn. (4) is the assumption that the soil description for the T_{15} layer(s) is reasonably known, and no substantial uncertainty exists about this input factor. However, if uncertainty does exist, the following section gives further guidance regarding the application of eqn. (4).

Application of the Modified MLR Model

Because the modified MLR model (eqn. (4)) and the Youd et al. (2002) MLR model (eqn. (1)) were derived from the same case history database, much of the following guidance for applying eqn. (4) is similar to that published in Bartlett and Youd (1992; 1995) and Youd et al. (2002). We offer additional guidance and recommendations herein; however, we strongly encourage readers to refer to Youd et al. (2002) for more details.

1. Similar to eqn. (1), predictions from eqn. (4) have more uncertainty when using input factors that are outside the range of the MLR database used to derive the partial regression coefficients. In short, eqn. (4) predicts D_H values generally within a factor of two for $6 \leq M \leq 8$ earthquakes at liquefiable sites underlain by continuous layers of sandy and silty sediments having topographical and soil conditions within the following ranges: $1 \leq W \leq 20\%$, $0.1 \leq S \leq 6\%$, $1 \leq T_{15} \leq 15$ m, $0.1 < T_{15,cs} \leq 10$ m.

2. Before applying eqn. (4), one should first decide if liquefaction is likely at the site for the design earthquake, and that the liquefiable layer(s) is relatively thick (i.e., $T_{15} > 1$ m) and shallow. From the MLR case history database, the depth to the top of the liquefiable layer was usually found in the upper 10 m of the soil profile and almost always found within the upper 15 m of the soil profile.

3. Numerous methods are readily available for determining liquefaction susceptibility (e.g., Cetin et al. 2004), and these methods are not further discussed in this paper. We leave it up to the practitioner, or regulatory agency, to decide what threshold level (i.e., factory of safety) to use to define if the soil is potentially liquefiable. If the site is deemed non-liquefiable, then significant ground displacement is not expected. If the site is considered liquefiable, then the practitioner should compute T_{15} according to the method described by Bartlett and Youd (1992). We emphasize that the calculation of the T_{15} variable is not a function of the factor of safety against triggering liquefaction, instead it is simply the cumulative thickness of saturated, cohesionless sediments having values of $N_{1,60} \leq 15$. Hence, T_{15} can be calculated independently of the factor of safety calculation for cases where liquefaction is expected at the candidate site.

4. It is also important to note that Bartlett and Youd (1992; 1995) found that sediments with values of $N_{1,60} > 15$ are generally resistant to lateral spreading for $M < 8$ earthquakes. The few exceptions in the case history database are related to the very large and long duration ($M = 9.2$) 1964 Alaska earthquake, where sediments with values of $N_{1,60}$ up to 20 displaced a maximum of 1 m. Because of the limited data for $M > 8$ earthquakes in the MLR case history database, eqn. (4) may not predict reliable displacements for such events.

5. When applying eqn. (4), one must select either free-face or ground-slope conditions in the model. If there is some question regarding the controlling topographical condition, then a conservative approach is to estimate D_H using both cases. Then we recommend the use of the case that produces the largest estimate of D_H. For sites with values of $W > 5\%$, free-face conditions generally control; whereas, for sites with $W < 1\%$, ground-slope conditions generally control. Because the MLR case history database is mostly comprised of sites where $W \leq 20\%$, eqn. (4) may be overly conservative when predicting displacements that are very close to a free-face (i.e., $W > 20\%$) where slumping or flow failure may occur. Similarly, eqn. (4) may underpredict displacements at steep sites (i.e., $S > 6\%$) where liquefaction may produce much larger ground displacement due to the presence of the steepened slope (e.g., flow failure).

6. As listed in Table 4, the majority of the T_{15} layers in the MLR case history database are described as sandy silts, silty sands, and fine-grained to very coarse-grained sands. Only 5 boreholes identified T_{15} layers generally described as silty gravel (i.e., $SI = 1$). More case history data are needed to fully verify eqn. (4) for gravelly sites with $SI = 1$.

7. Like eqn. (1), eqn. (4) is appropriate for estimating horizontal displacement at stiff soil sites in the Western U.S. and Japan where attenuation of strong ground motion with distance

from the seismic source is fairly high. Youd et al. (2002) presented a method to adjust *R* to account for differing crustal attenuation relationships in other seismic regions (e.g., Eastern U.S.) or for sites underlain by soft soils.

8. Eqn. (4) includes soil description factors which are reasonably reliable. However, soil descriptions from existing borehole logs may have additional uncertainty, if field investigations have not been performed by qualified and trained personnel. As discussed earlier, we verified that the soil descriptions in the MLR database correspond to recorded values of fines content and mean grain size; hence, additional uncertainty due to incorrect visual soil descriptions is not included in the standard deviation of the predicted variable, σ_{logDH}, of eqn. (4). To address this issue, we recommend the following approach. (I) For new investigations/evaluations and if laboratory testing is possible, we recommend the use of the Youd et al. (2002) MLR model because it requires laboratory determined measurements of $D50_{15}$ and F_{15}. (We do not intend that our model supplants nor updates the work of Youd et al., (2002).) (II) For new investigations/evaluations and if laboratory testing is not always desired, a prudent approach is to test the skill of the field investigator by occasionally performing random laboratory measurements and comparing them with the investigator's soil descriptions. Random errors in the investigator's descriptions could then be modeled by simulation. (III) For evaluations requiring the use of existing borehole data, the practitioner should decide whether or not the soil descriptions on the soil logs are sufficiently reliable. This evaluation should be made based on the source of the data and the qualifications and care of the field personnel. We believe that trained personnel can make reasonably reliable field descriptions of soil type, if trained in the procedures of ASTM D2488-9a (ASTM 2009). (IV) If the soil description(s) of the T_{15} layer(s) is still

deemed to be uncertain, then either a conservative estimate of the soil description can be made, or eqn. (3) can be applied which does not require soil description inputs (and has a higher value of σ_{logD_H}). For example, if questions arise about whether or not the critical layer is a silty sand or a sandy silt, then the evaluator might use the silty sand description because this would produce a more conservative (i.e., higher) estimate of horizontal displacement. If a layer is described as "sandy silt with seams of sand", we recommend the assignment of an *SI* value equal to 4, not 5. Similarly, if a layer is described as "fine-grained sand with some silt", one might assign the layer a value of *SI* equal to 3, not 4. An even more conservative approach is to assign *SI* = 3 to all sandy layers, and *SI* = 4 to silty sandy layers.

9. As shown in Figure 1b, estimates of lateral spread displacement from eqn. (4) are generally accurate within plus or minus a factor of 2. If a conservative estimate is desired, then we recommend that the evaluator multiply D_H obtained from eqn. (4) by a factor of 2 for an estimate that is not likely to be greatly exceeded.

10. Significant or large estimates of lateral spread displacement obtained from eqn. (4) should be further validated by performing additional subsurface investigations, geotechnical in-situ tests, laboratory testing, and displacement analyses. During such investigations, investigators should collect the necessary data for use in more comprehensive analyses and modeling.

Evaluations Using CPT Data

The Cone Penetration Test (CPT) has become very popular for site investigations because it is generally faster, more repeatable, and more economical than traditional site investigation

methods, such as drilling and sampling (Robertson 2009). While assessing lateral spreading hazards for the aforementioned study in Weber County, Utah, we obtained data from 157 CPT soundings recorded in the offices of numerous municipalities, private engineering firms, and state governments (Bartlett and Gillins, 2013). Because of the abundance of CPT data, we desired to use it to estimate the geotechnical inputs in the MLR model; thereby enabling development of distributions of $T_{15,cs}$ for various mapped geologic units, and application of the MLR equations to estimate lateral spread displacements at the CPT sounding sites.

Data from the CPT cannot be used to reliably estimate the mean grain size and fines content variables, as needed in the Youd et al. (2002) MLR model. However, the CPT does provide near continuous data with depth that can be used to identify soil stratigraphy and soil type, as required in the modified MLR model (eqn. (4)). In the following sections, a simple procedure is presented to classify the soil for use in eqn. (4) and to convert CPT penetration data to equivalent SPT N values. We show that such conversions are reasonable using a dataset of paired SPT-CPT borehole/soundings obtained from Holocene and late Pleistocene granular deposits in northern Utah (i.e., Weber County). However, the analyses presented in this section are specific to our study area and must be validated for use at other locales. Relationships between soil type and SPT and CPT data can be affected by many factors (e.g., geologic depositional environment, parent mineralogy, and age and cementation of the sediments). Nonetheless, we believe that practitioners may readily follow the process presented herein to develop or validate their own correlations (or correlations developed by others) for possible application, as deemed appropriate.

Estimating soil description variables from CPT Data

Numerous researchers have developed charts that relate CPT data, such as tip resistance and friction ratio, to soil type or soil behavior type (e.g., Schmertmann 1978, Douglas and Olsen 1981, Olsen and Malone 1988, Robertson et al. 1986, Robertson 1990, Jefferies and Davies 1991). Robertson (1990) introduced one of the most widely used CPT-based charts to define soil behavior type. This chart links normalized CPT tip resistance, Q_{tn}, and normalized friction ratio, F_r, to the in situ mechanical soil behavior, named the "normalized soil behavior type" (SBTn). Often, soil classification, such as the USCS which is based on grain-size distribution and plasticity of disturbed samples, relates well with CPT-based SBTn (e.g., Molle 2005).

Jefferies and Davies (1993) introduced an index to define the soil behavior type, named the Soil Behavior Type Index, I_c. This index is simply the radius of concentric circles which plot on Jefferies and Davies (1991) SBTn chart. Robertson and Wride (1998) modified the definition of I_c such that certain values of I_c will approximate the boundaries of SBTn zones 2-7 on the Robertson (1990) Q_t - F_r SBTn chart (see base layer of Figure 4). Zhang et al. (2002) most recently updated the definition of I_c, which is shown in eqn. (8).

$$I_c = [(3.47 - LogQ_{tn})^2 + (LogF_r + 1.22)^2]^{0.5} \quad (8)$$

Jefferies and Davies (1993) suggested that I_c could be used to develop empirical correlations of CPT-based data that vary with soil type. With this in mind, we compiled available "pairs" of side-by-side SPT borings and CPT soundings from the study area in Weber County, Utah, into a database. From this, there are 205 samples that were classified according to the USCS from laboratory measurements. Based on these evaluations, we assigned the samples

values of *SI*, as defined in Table 3. In addition, at the depth intervals where these samples were taken, we found the median values of Q_{tn}, F_r, and I_c from the adjacent CPT soundings. Figure 4 plots these CPT data, symbolized by *SI*, on the Robertson (1990) Q_t - F_r SBTn chart. (We note that the Weber County database lacks samples with *SI* = 2, but the method presented below could be extended to include this soil type, if the database were expanded.)

Figure 5 shows histograms of I_c, grouped by *SI*, from the Weber County database. A normal probability density function is fitted to each dataset. Table 6 lists the mean and standard deviation ($\overline{I_c}$ and s_{Ic}, respectively) of I_c for each *SI* along with results of a Lilliefors' goodness-of-fit test for normality. A Lilliefors' test is a special type of the Kolmogorov-Smirnov (K-S) statistical test used to test the null hypothesis that data come from a normally distributed population where the mean and standard deviation parameters are estimated rather than fully known (such as due to a small sample size). Because the computed *P*-values are greater than the 5% significance level, the null hypothesis that the data are normally distributed cannot be rejected.

With some confidence that the groups are normally distributed, we next verified that I_c statistically discriminates between each group of *SI*. A one-way ANOVA test rejects the global null hypothesis that the means, $\overline{I_c}$, are the same across the groups of *SI* at the 5% significance level. We then used multiple comparison procedures to determine if the means differ between groups. Figure 6 graphically displays the results of the comparison using the Tukey—Kramer single-step method at the 5% significance level. Because none of the horizontal lines of each group overlap, the means of each group are statistically different. We conclude that in terms of the means of each group of *SI*, I_c appears to be a reasonable discriminator of soil type.

Due to small sample sizes and similar variances of I_c for SI =1 and SI =3, we performed a two-sample F-test of the hypothesis that these two groups come from normal distributions with the same variance. The test finds that the F-statistic = 1.208, and the P-value = 0.841; therefore, the null hypothesis cannot be rejected at the 5% significance level. The pooled variance of I_c for SI =1 and SI =3 is 0.036; and, the pooled standard deviation, s_{Ic}, is 0.190.

If it is assumed that each of the soil types have the same probability of being encountered randomly in situ, then eqn. (9) is true for determining the probability of a particular soil index, $P(SI = i)$, given a value of I_c.

$$P(SI = i \mid I_c) = \frac{N(\overline{I_{ci}}, s_{Ici}^2)}{\sum_{i=1}^{M} N(\overline{I_{ci}}, s_{Ici}^2)} \tag{9}$$

where N is the normal probability density function of I_c, with mean = $\overline{I_c}$ and variance = s^2_{Ic}, for the particular $SI = i$. Zhang and Tumay (1999) developed this equation rigorously for the soil classification index, U, rather than for I_c.

Figure 7 displays the recommended normal probability density functions of I_c for each SI based on the data from Weber County, Utah. Figure 8 depicts the graphical solution of eqn. (9) for each SI using the normal probability density functions in Figure 7.

Eqn. (9) (or Figure 8) provides a method to estimate the probability of each SI for a specific I_c value from the associated conditional probability density functions. For example, if a layer of soil has a value of I_c = 2.0, then P_1 = 0.01, P_3 = 0.42, P_4 = 0.47, P_5 = 0.10, and P_6 = 0.00, where P_i is the conditional probability that $SI = i$. If that same soil was considered susceptible to both liquefaction and lateral spreading, then the values of P_1, P_3, P_4, and P_5, could be inserted

into eqn. (4) as variables x_1, x_3, x_4, and x_5, respectively, for that layer. Once again, soils with SI = 6 were not considered to be susceptible to liquefaction.

Estimating T_{15} with CPT Data

Numerous researchers have found correlations between SPT N values and CPT cone tip resistance, q_t (e.g., Robertson et al. 1983, Robertson and Campanella 1986, Kulhawy and Mayne 1990, Jefferies and Davies 1993). In the aforementioned SPT-CPT "pairs" database for Weber County, Utah, there are 327 samples with SPT N values corrected to an energy ratio of 60%, N_{60}. Across the 0.3 meters of depth where these blow counts were measured, we found the median values of q_t, and I_c from the adjacent CPT soundings. These points are plotted in Figure 9. Values of q_t are made dimensionless by dividing by the atmospheric pressure, P_a. As can be seen, there is a negative correlation between the $Log\ [(q_t / P_a) / N_{60})]$ versus I_c.

Robertson and Wride (1998) suggested that the approximate boundary between cohesionless and cohesive behavior for a soil is around I_c = 2.60. After performing an initial linear regression, we noted 5 data points that have values of $I_c > 2.60$, and that deviated from the regressed line more than three standard deviations. These 5 data points are circled in Figure 9, and are considered outliers.

After removal of the 5 outliers, linear regression of the remaining 322 data points gives the relationship shown in eqn. (10).

$$Log[(q_t / P_a) / N_{60})] = 1.25 - 0.289 \cdot I_c \qquad (10)$$

497 This regression model has a value of R^2 equal to 65.9%, and a standard deviation of the
498 predicted variable equal to 0.139.

499 Because of the noted outliers in the cohesive area of Figure 9, this relationship is more
500 tenuous and not recommended when $I_c > 2.60$. However, when studying liquefaction and lateral
501 spread, we are concerned with saturated, *cohesionless* sediments. The relationship presented in
502 eqn. (10) appears more reliable in the cohesionless area of Figure 9.

503 After finding N_{60} from eqn. (10) and correcting it for overburden stress to $N_{1,60}$, layers in
504 the upper 15 meters of the CPT logs that are saturated, cohesionless, and have values of $N_{1,60} \leq$
505 15 are identified. T_{15} is found by summing the thickness of these layers.

506 Eqn. (9) is used to compute the conditional probabilities of *SI* (P_1, P_3, P_4, and P_5) from
507 values of I_c for each of these layers. The averages of these conditional probabilities can then be
508 inserted into eqn. (4) as the variables x_1, x_3, x_4, and x_5 (per eqn. (11)).

509

510 $$x_i = \frac{T_{15}}{\sum_{j=1}^{m} \frac{t_j}{P_i}} \qquad (11)$$

511

512 where t_j is the thickness of the *j*-th layer that comprises T_{15} at the CPT sounding (m) and P_i is the
513 conditional probability that $SI = i$ for the *j*-th layer.

514

515 **Conclusions**

516 1. The Youd et al. (2002) MLR empirical model for predicting horizontal displacement from
517 liquefaction-induced lateral spread requires specific inputs from laboratory testing, namely
518 mean grain size, $D50_{15}$, and average fines content, F_{15}. Some investigators who are

519 performing large-scale (e.g., regional hazard mapping) or preliminary lateral spread studies
520 may wish to estimate inputs in this empirical model using existing or record geotechnical
521 borehole data. Unfortunately, many practitioners performing routine drilling and sampling
522 commonly report the soil description and thickness (and SPT blow count (N) values) of
523 individual layers with depth, but rarely report mean grain size and fines content data with
524 depth. To overcome this lack of available data, this paper proposes to replace the $D50_{15}$
525 and F_{15} variables in the MLR model with soil description variables. Remarkably, the
526 resulting modified MLR model (eqn. (4)) has a coefficient of determination, R^2, equal to
527 79.0%, only 4.6% less than R^2 for the Youd et al. (2002) empirical model (eqn. (1)).

528 2. The proposed model does not replace that of Youd et al. (2002). Rather, the proposed
529 model provides a method for estimating lateral spread displacement from existing borehole
530 data that lacks measurements of mean grain size and fines content, but has reliable
531 descriptions of soil type for the layers comprising T_{15}. Once these estimates have been
532 made, investigators should then decide if new drilling and sampling is warranted in order to
533 further reduce the uncertainties in the subsurface, and improve the estimates of lateral
534 spread displacement.

535 3. Fine to medium-grained sands with low fines content are associated with larger lateral
536 spread displacement than coarse grained sands, silty sands, sandy silts, or fine gravels.
537 This can be seen from the partial regression coefficients of the soil description variables of
538 eqn. (4).

539 4. Data from the CPT cannot be reliably used to estimate mean grain size and fines content, as
540 needed in the Youd et al. (2002) MLR model, but such data can be used to identify soil
541 stratigraphy and soil type, as needed in the proposed modified MLR model (eqn. (4)). This

paper presented a procedure to adapt CPT data for use in eqn. (4). We show that such conversions are reasonable using a dataset of paired SPT-CPT borehole/soundings obtained from Holocene and late Pleistocene granular deposits in northern Utah (i.e., Weber County). However, the analyses presented herein were specific to our study area and must be validated for use at other locales. Nonetheless, we believe that practitioners may readily follow the process to develop or validate their own correlations (or correlations developed by others) for possible application, as deemed appropriate.

5. The modified MLR model (eqn. (4)) may be particularly useful for investigators engaged in large-scale lateral spreading hazard studies using existing or available geotechnical borehole data which lack measurements of $D50_{15}$ and F_{15}. Bartlett and Gillins (2013) shows how this model can be applied to create regional hazard maps depicting the probability of lateral spread displacements exceeding threshold distances.

6. Future work should compile newer case histories of lateral spreading in order to expand the MLR database and further test the performance of the empirical models and the proposed procedure for adapting CPT data. Many newer case histories have higher quality laboratory and field data than the case histories listed in Table 4. Updates of the regressions to include newer case history data may also expand the recommended range of the input variables in the empirical models to other soil conditions (e.g., gravelly soils, different geographic locations), and seismic loading conditions (e.g., earthquakes greater than magnitude 8).

References

American Society for Testing and Materials (ASTM) (2009). "Standard Practice for Description and Identification of Soils (Visual-Manual Procedure)." *ASTM D2488-09a*, July 2009, originally approved in 1966, 12 pp.

Bardet, J. P., Tobita, T., Mace, N., and Hu, J. (2002). "Regional modeling of liquefaction-induced ground deformation." *Earthquake Spectra* 18(1), 19-46.

Bartlett, S. F., and Gillins, D. T. (2013). "Mapping the probability and uncertainty of liquefaction-induced ground failure for Weber County, Utah." *U.S.G.S. External Research Award No. G12AP20074*, Earthquake Hazards Program, Denver, CO, 295 pp.

Bartlett, S. F., and Youd, T. L. (1992). "Empirical Analysis of Horizontal Ground Displacement Generated by Liquefaction-Induced Lateral Spreads." *Technical Report NCEER-92-0021*, National Center for Earthquake Engineering Research, Buffalo, NY.

Bartlett, S. F., and Youd, T. L. (1995). "Empirical prediction of liquefaction-induced lateral spread." *J. Geotech. Eng*. 121(4), 316-328.

Baska, D. A. (2002). "An Analytical/Empirical Model for Prediction of Lateral Spreading Displacements." *Ph.D. Dissertation*, University of Washington, Seattle, WA, 539 pp.

Cetin, K. O., Seed, R. B., Kiureghian, A. D., Tokimatsu, K., Harder, L. F., Jr., Kayen, R. E., and Moss, R. E. (2004). "Standard Penetration Test-based probabilistic and deterministic assessment of seismic soil liquefaction potential." *J. Geotech. Geoenviron. Eng.* 130(12), 1314 – 1340.

Douglas, B. J., and Olsen, R. S. (1981). "Soil classification using electric cone penetrometer." *Cone Penetration Testing and Experience, Proc. of a Session, ASCE National Convention*, G. M. Norris and R. D. Hotz (editors), St. Louis, MO, pp. 209–227.

585 Faris, A. T., Seed, R. B., Kayen, R. E., and Wu, J. (2006). "A Semiempirical Model for the
586 Estimation of Maximum Horizontal Displacement due to Liquefaction-Induced Lateral
587 Spreading." *Proc. 8th U.S. Conference on Earthquake Engineering*, vol. 3, paper no. 1323,
588 San Francisco, CA, pp. 1584-1593.
589 Hamada, M., Yasuda, S., Isoyama, R., and Emoto, K. (1986). "Study on liquefaction induced
590 permanent ground displacements." *Report for the Association for the Development of*
591 *Earthquake Prediction in Japan,* Tokyo, Japan, 87 pp.
592 Jefferies, M. G., and Davies, M. P. (1991). "Soil classification by the cone penetration test:
593 discussion." *Canadian Geotechnical Journal* 28(1), 173–176.
594 Jefferies, M. G., and Davies, M. P. (1993). "Use of CPTU to estimate equivalent SPT N60."
595 *Geotechnical Testing Journal* 16(4), 458–468.
596 Kulhawy, F. H., and Mayne, P. H. (1990). "Manual on Estimating Soil Properties for Foundation
597 Design." *EL-6800, Research Project 1493-6,* Electric Power Research Institute (EPRI), Palo
598 Alto, CA.
599 Molle, J. (2005). "The Accuracy of the Interpretation of CPT-Based Soil Classification Methods
600 in Soft Soils." *M.Sc. Thesis*, Delf University of Technology, Delft, the Netherlands.
601 National Research Council (NRC) (1985). *Liquefaction of soils during earthquakes*. National
602 Academy Press, Washington D.C., 240 pp.
603 Olsen, M. J., Bartlett, S. F., and Solomon, B. J. (2007). "Lateral spread hazard mapping of the
604 Northern Salt Lake Valley, Utah for a M7.0 scenario earthquake." *Earthquake Spectra* 23(1),
605 95-113.

606 Olsen, R. S., and Malone, P. G. (1988). "Soil Classification and site characterization using the
607 cone penetrometer test." *Penetration Testing 1988, Proc. of the 1st Int. Conf. on Penetration*
608 *Testing, ISOPT-l*, J. de Ruiter (editor), vol. II, Orlando, FL, pp. 887-893.
609 Olson, S. M., and Johnson, C. I. (2008). "Analyzing liquefaction-induced lateral spreads using
610 strength ratios." *J. Geotech. Geoenviron. Eng.* 134(8), 1035-1049.
611 Rauch, A. F., and Martin, J. R. (2000). "EPOLLS model for predicting average displacements
612 on lateral spreads." *J. Geotech. Geoenviron. Eng.* 126(4), 360-371.
613 Robertson, P.K. (1990). "Soil classification using the cone penetration test." *Canadian*
614 *Geotechnical Journal* 27(1), 151–158.
615 Robertson, P. K. (2009). "Soil behaviour type from the CPT: an update." *Gregg Drilling &*
616 *Testing Inc.*, Signal Hill, CA, 8 pp.
617 Robertson, P. K., and Campanella, R. G. (1983). "Interpretation of the cone penetrometer test:
618 parts I-II." *Canadian Geotechnical Journal* 20(4), 718-745.
619 Robertson, P. K., Campanella, R. G., Gillespie, D., and Greig, J. (1986). "Use of piezometer
620 cone data." *Proc. of In Situ '86, a Specialty Conf. Sponsored by the Geotechnical Eng.*
621 *Division of the ASCE*, GSP No. 6, S. P. Clemence (editor), Blacksburg, VA, pp. 1263-1280.
622 Robertson, P.K., and Wride, C.E. (1998). "Evaluating cyclic liquefaction potential using the
623 cone penetration test." *Canadian Geotechnical Journal* 35(3), 442–459.
624 Schmertmann, J. H. (1978). "Guidelines for Cone Penetration Test, Performance and Design."
625 *Report FHWA-TS-78-209*, US Federal Highway Administration, Washington D.C., 145 pp.
626 Youd, T. L., Hansen, C. M., and Bartlett S. F. (2002). Revised multilinear regression equations
627 for prediction of lateral spread displacement." *J. Geotech. Geoenviron. Eng.* 128(12), 1007-
628 1017.

629 Youd, T.L., and Perkins, D. M. (1987). "Mapping of liquefaction severity index." *J. Geotech.*
630 *Eng.* 113(11), 1374-1392.
631 Zhang, G., Robertson, P. K., and Brachman, R. W. I. (2002). "Estimating liquefaction-induced
632 ground settlements from CPT for level ground." *Canadian Geotechnical Journal* 39(5),
633 1168-1180.
634 Zhang, G., Robertson, P. K., and Brachman, R. W. (2004). "Estimating liquefaction-induced
635 lateral displacements using the standard penetration test or cone penetration test." *J.*
636 *Geotech. Geoenviron. Eng.* 130(8), 861-871.
637 Zhang, Z., and Tumay, M. (1999). "Statistical to fuzzy approach toward CPT soil
638 classification." *J. Geotech. Geoenviron. Eng.* 125(3), 179-186.

Table 1. ANOVA results of eqn. (1)

Source of Variation	Sum of Squares	Deg. of Freedom	Mean Squares
Regression	93.53	9	10.3923
Error	18.39	474	0.0388
Total	111.92	483	

F-statistic = 267.9; P-value = 0.000; $\overline{R^2} = 83.3\%$

Table 2. ANOVA results of eqn. (3)

Source of Variation	Sum of Squares	Deg. of Freedom	Mean Squares
Regression	74.56	7	10.6520
Error	37.35	476	0.0785
Total	111.92	483	

F-statistic = 135.7; P-value = 0.000; $\overline{R^2} = 66.1\%$

Table 3. Descriptions and distributions of T_{15} layers in Youd et al. (2002) database

Typical Soil Descriptions in Database	*SI*	*n*	$\overline{D50}$ (mm)	σ_{D50} (mm)	$\overline{FC}$ (%)	σ_{FC} (%)	General USCS Symbol
Silty gravel with sand, silty gravel, fine gravel	1	5	6.45	4.28	19.9	5.6	GM
Very coarse sand, sand and gravel, gravelly sand	2	8	2.11	0.77	6.8	6.3	GM-SP
Coarse sand, sand with some gravel	2	33	0.63	0.18	7.3	4.5	SP
Sand, medium to fine sand, sand with some silt	3	80	0.34	0.02	4.8	2.4	SP-SM
Fine sand, sand with silt	4	50	0.17	0.04	14.6	11.0	SM
Very fine sand, silty sand, dirty sand, silty/clayey sand	4	41	0.10	0.03	37.0	11.3	SM-ML
Sandy silt, silt with sand	5	34	0.07	0.08	61.2	9.4	ML
Nonliquefiable material (not part of T_{15})	6	--	--	--	--	--	CL

Table 4. Earthquakes and displacement vectors in the Youd et al. (2002) case history database

Earthquake Name	Number of displacement vectors	Number of SPT boreholes that identified T_{15} layers with values of SI = 1,2,3,4, or 5				
		SI = 1	SI = 2	SI = 3	SI = 4	SI = 5
1906 San Francisco, California	2	-	-	2	4	-
1964 Alaska	7	-	10	1	7	3
1964 Niigata, Japan	299	-	24	61	47	11
1971 San Fernando, California	23	-	-	-	15	5
1979 Imperial Valley, California	31	-	-	-	8	6
1983 Borah Peak, Idaho	4	4	-	-	-	-
1983 Nihonkai-Chubu, Japan	72	-	-	16	-	-
1987 Superstition Hills, California	6	-	-	-	9	9
1989 Loma Prieta, California	2	-	2	-	-	-
1995 Hyogo-Ken Nanbu (Kobe), Japan	19	1	5	-	1	-
Total =	465	5	41	80	91	34

Table 5. ANOVA results of eqn. (4)

Source of Variation	Sum of Squares	Deg. of Freedom	Mean Squares
Regression	88.46	12	7.3717
Error	23.46	471	0.0498
Total	111.92	483	

F-statistic = 148.0; P-value = 0.000; $\overline{R^2} = 78.5\%$

Table 6. Lilliefors' goodness-of-fitness test results for normality

SI	n	$\overline{I_c}$	s_{Ic}	P-value	k Stat.	critical value
1	17	1.42	0.195	0.084	0.197	0.208
3	8	1.76	0.178	0.056	0.283	0.286
4	46	2.09	0.357	0.546	0.085	0.129
5	19	2.53	0.279	0.422	0.141	0.199
6	115	3.05	0.219	0.143	0.075	0.084

Figure 1
Click here to download Figure: Figure 1.pdf

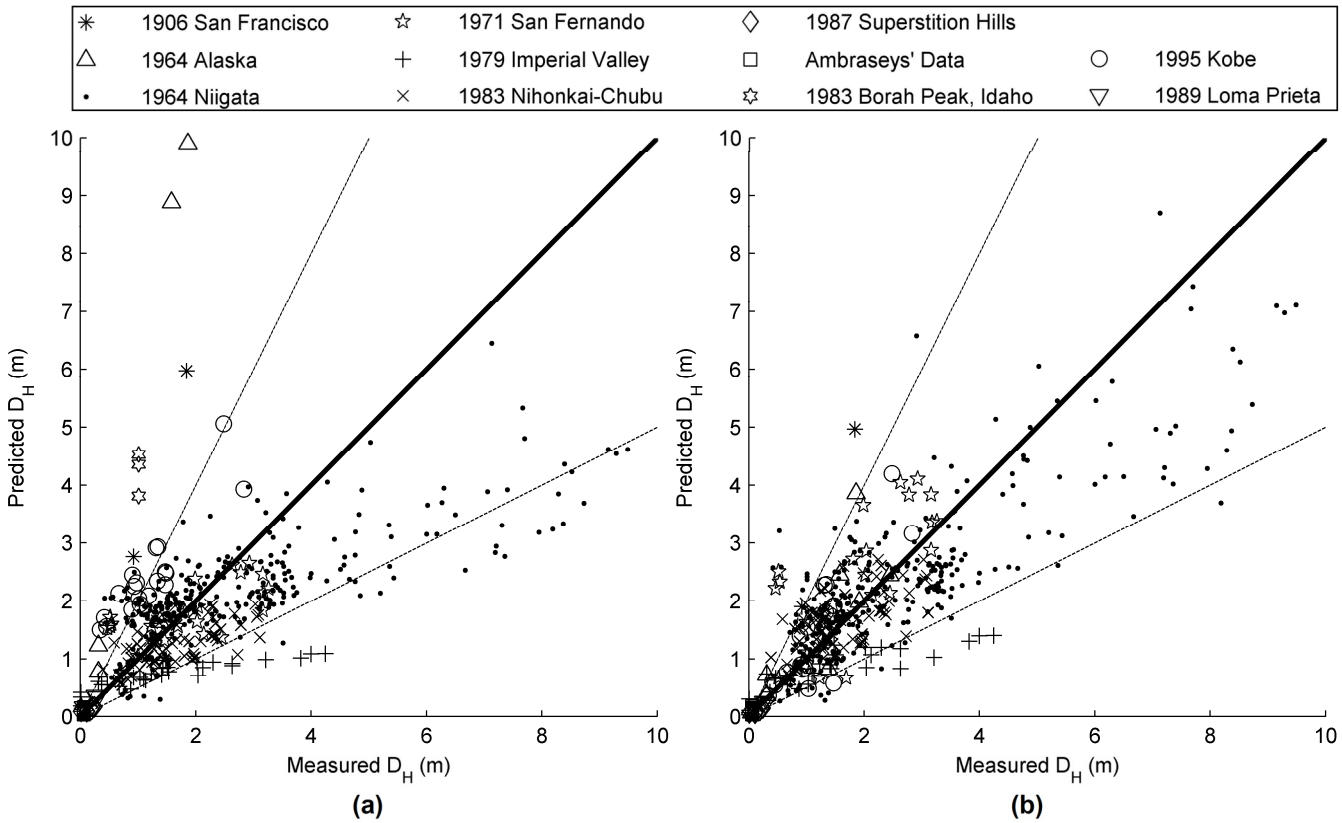

Figure 1. Predicted lateral spreading displacement using (a) eqn. (3), or (b) eqn. (4), versus measured lateral spreading displacement from the case history database of Youd et al., 2002

Figure 2
Click here to download Figure: Figure 2.pdf

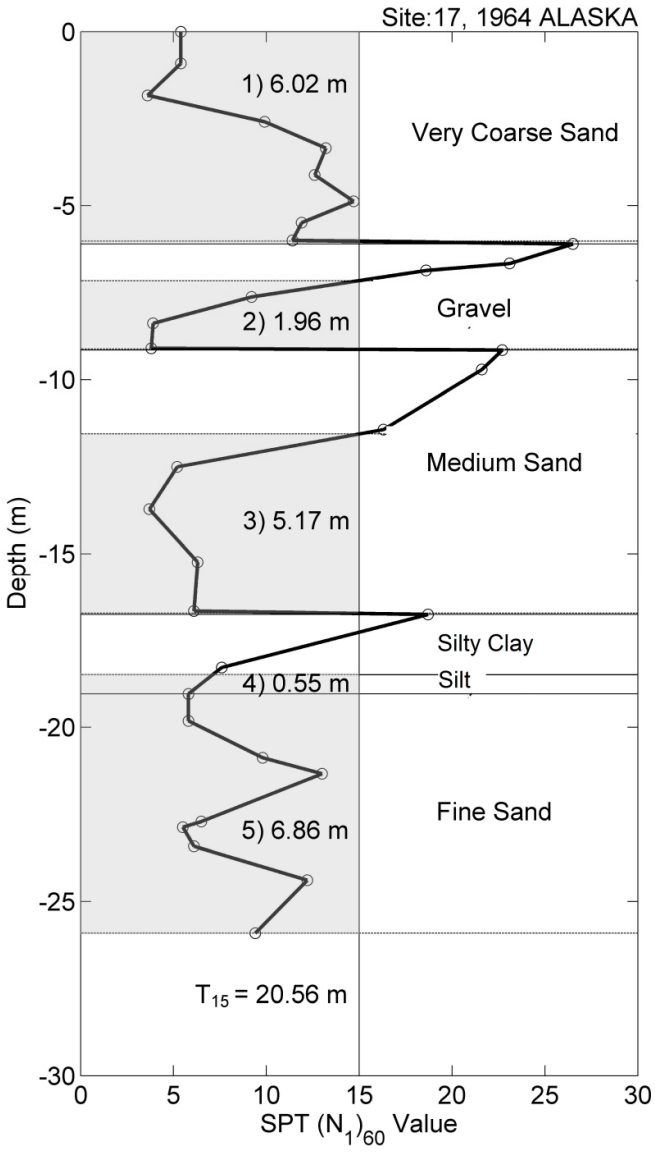

Figure 2. Boring log at Railroad Bridge Milepost 147.4, Matanuska River, Alaska. The five shaded layers comprise T_{15} at this site

Figure 3
Click here to download Figure: Figure 3.pdf

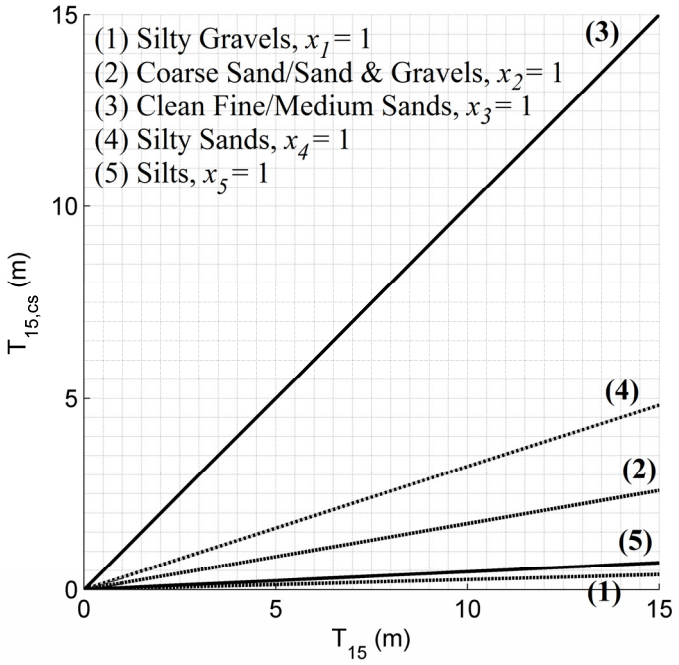

Figure 3. T_{15} vs. $T_{15,cs}$ according to soil index

Figure 4
Click here to download Figure: Figure 4.pdf

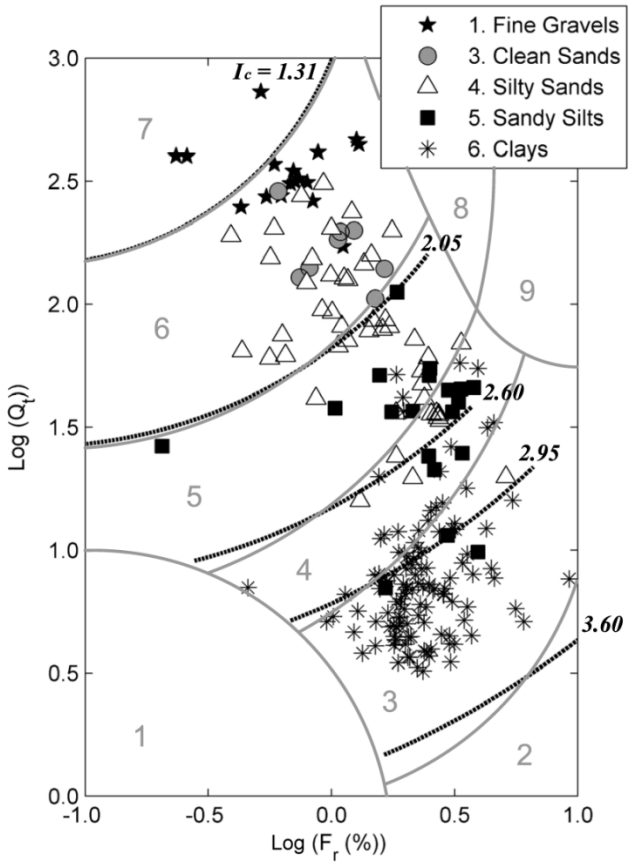

Figure 4. Data from Weber County, Utah, plotted on Robertson (1990) Q_t - F_r SBTn chart with contours of I_c

Figure 5
Click here to download Figure: Figure 5.pdf

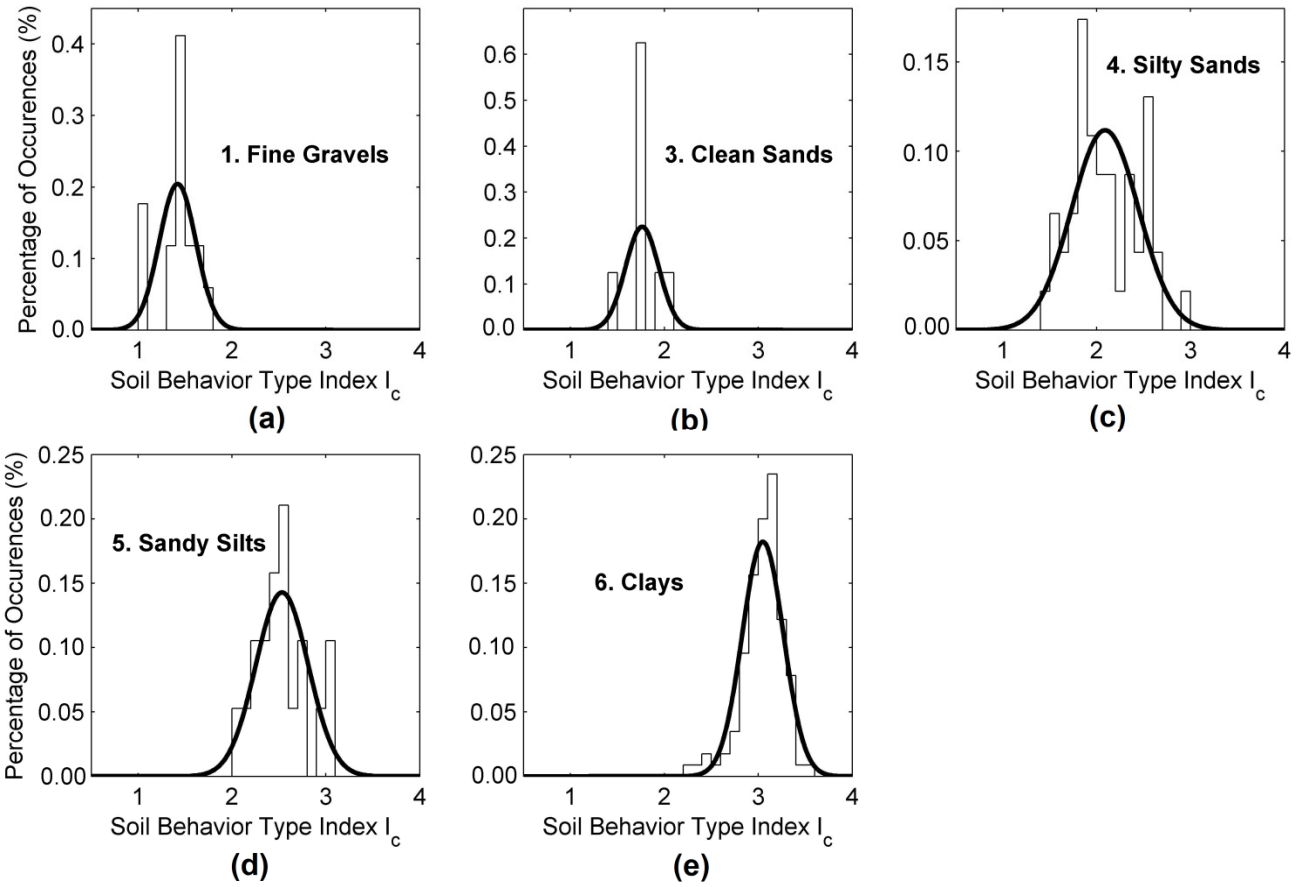

Figure 5. Histograms of I_c and fitted normal probability density functions for (a) $SI = 1$, (b) $SI = 3$, (c) $SI = 4$, (d) $SI = 5$, (e) $SI = 6$; data from Weber County, Utah

Figure 6
Click here to download Figure: Figure 6.pdf

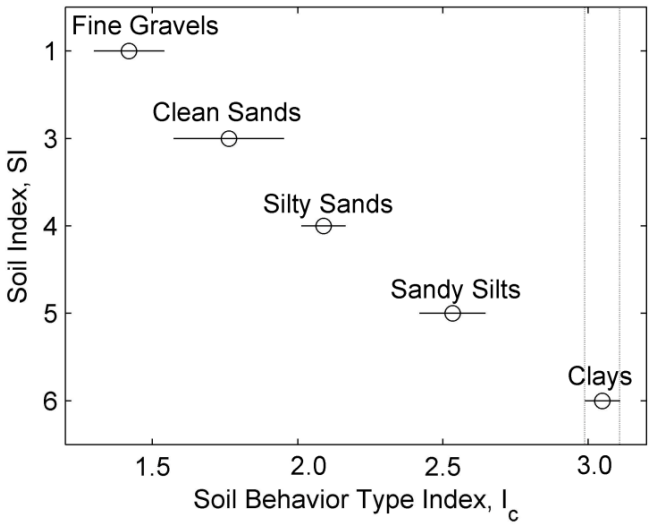

Figure 6. Multiple comparisons of the means of I_c, grouped by *SI*; data from Weber County, Utah

Figure 7
Click here to download Figure: Figure 7.pdf

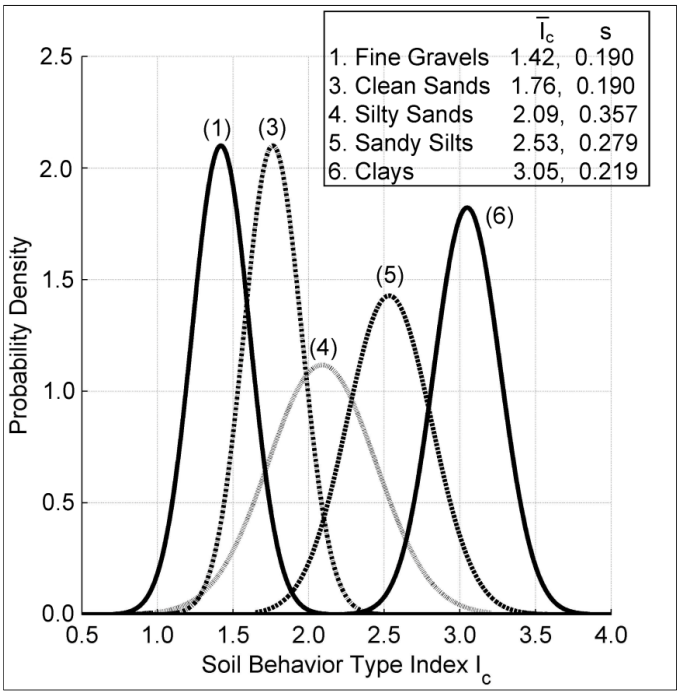

Figure 7. Recommended normal probability density functions for I_c, grouped by *SI*; Weber County, Utah

Figure 8
Click here to download Figure: Figure 8.pdf

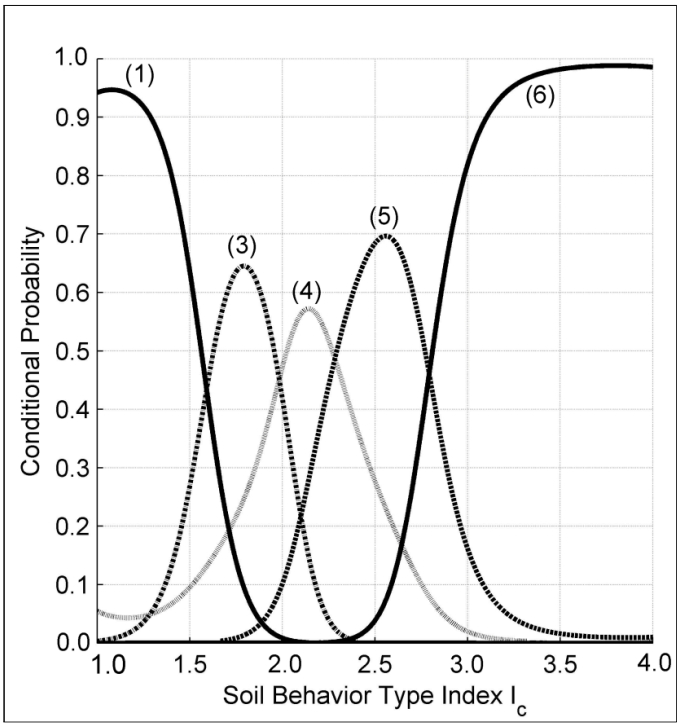

Figure 8. CPT point estimation chart for *SI* given I_c; Weber County, Utah

Figure 9
Click here to download Figure: Figure 9.pdf

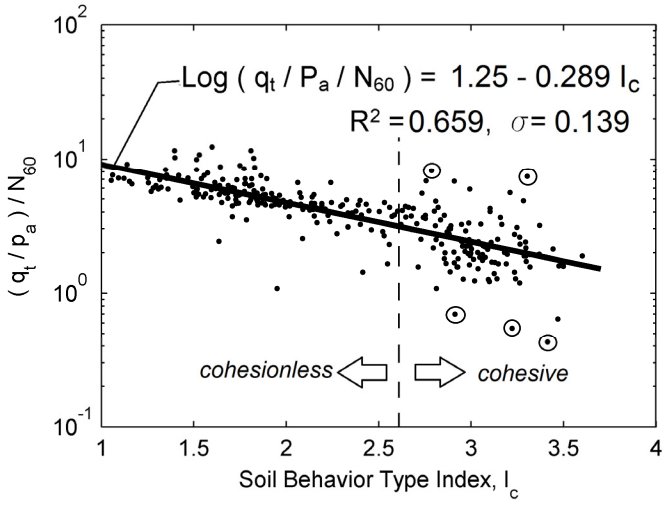

Figure 9. Relationship between CPT-data and SPT N_{60}; Weber County, Utah. Circled data points considered outliers (not used in the regression).

Figure Captions:

Figure 1. Predicted lateral spread displacement using (a) eqn. (3), or (b) eqn. (4), versus measured lateral spread displacement from the case history database of Youd et al., 2002

Figure 2. Boring log at Railroad Bridge Milepost 147.4, Matanuska River, Alaska. The five shaded layers comprise T_{15} at this site

Figure 3. T_{15} vs. $T_{15,cs}$ according to soil index

Figure 4. Data from Weber County, Utah, plotted on Robertson (1990) Q_t - F_r SBTn chart with contours of I_c

Figure 5. Histograms of I_c and fitted normal probability density functions for (a) SI = 1, (b) SI = 3, (c) SI = 4, (d) SI = 5, (e) SI = 6; data from Weber County, Utah

Figure 6. Multiple comparisons of the means of I_c, grouped by SI; data from Weber County, Utah

Figure 7. Recommended normal probability density functions for I_c, grouped by SI; Weber County, Utah

Figure 8. CPT point estimation chart for SI given I_c; Weber County, Utah

Figure 9. Relationship between CPT-data and SPT N_{60}; Weber County, Utah. Circled points are considered outliers.